Dyke Award

Evaluation of Contrast-Enhanced MR Imaging in a Brain-Abscess Model

Val M. Runge[1]
Jeffrey A. Clanton[1]
Ann C. Price[1]
Willam A. Herzer[2]
Joseph H. Allen[1]
C. Leon Partain[1]
A. Everette James, Jr.[1]

An alpha-streptococcus brain abscess was produced in five dogs and studied with magnetic resonance (MR) imaging (0.5 T) and computed tomography (CT). Non-contrast- and contrast-enhanced CT scans were obtained using gadolinium diethylenetriamine-pentaacetic acid (Gd DTPA) for MR imaging and meglumine iothalamate for CT scanning. Each animal was evaluated in the early and later cerebritis stages of abscess evolution. On MR, the area of cerebritis enhanced after administration of Gd DTPA in a manner similar to that observed with contrast-enhanced CT. However, contrast enhancement was greater on the MR examination. Early lesions in two animals were detected only with contrast-enhanced MR imaging. This experience suggests that intravenously administered agents such as Gd DTPA should increase the diagnostic potential of MR imaging in neurologic diseases, especially those altering the blood-brain barrier.

Magnetic resonance (MR) imaging has rapidly progressed from the stage of development as a laboratory instrument to implementation as a diagnostic technique for neurologic disease [1–8]. The lack of ionizing radiation, the direct multiplanar imaging capability, the lack of bone artifact, and the inherent sensitivity to pathologic change have prompted rapid acceptance of this imaging technique. The inability to separate magnetically similar but histologically different tissues, such as neoplasia or abscess, from surrounding edema, has remained a shortcoming in neurologic use, thus indicating an important role for MR contrast agents [1, 9–11]. Despite the significance of this clinical problem, few experimental studies have been pursued [12–14]. Previous investigations were limited in scope by both the number of animals used and the MR imaging techniques employed.

A canine brain-abscess model [15] was used to evaluate the relative efficacy of MR imaging and computed tomography (CT) in the detection and characterization of this lesion. Primary emphasis was placed on elucidating the potential role of intravascular MR contrast media. In our study, a contrast agent with significant potential for human application, gadolinium diethylenetriaminepentaacetic acid (Gd DTPA), was tested. The toxicity of this compound approaches that of conventional iodinated agents [16]. Its strong proton relaxation at low concentrations and high in vivo stability have made possible the initiation of clinical trials in Europe. Excretion is primarily renal with greater than 90% recovery by 24 hr. The use of an agent such as Gd DTPA [17] may enable precise localization of blood-brain barrier (BBB) breakdown on MR imaging.

Materials and Methods

Experimental Model

An alpha-steptococcus brain abscess was produced by a previously described method [15] in five mongrel dogs weighing 6–28 kg. For the surgical procedure and imaging (CT and MR), the dogs were anesthetized with intravenous pentobarbital (25 mg/kg) and intubated. Surgery was performed under aseptic conditions. After reflection of the dorsal musculature,

Received July 2, 1984; accepted after revision September 20, 1984.

Presented at the annual meeting of the American Society of Neuroradiology, Boston, June 1984.

[1] Department of Radiology and Radiological Sciences, Vanderbilt University Medical Center, Nashville, TN 37232. Address reprint requests to A. E. James, Jr.

[2] Department of Pharmacology, Vanderbilt University Medical Center, Nashville, TN 37232.

***AJNR* 6:139–147, March/April 1985**
0195–6108/85/0602–0139

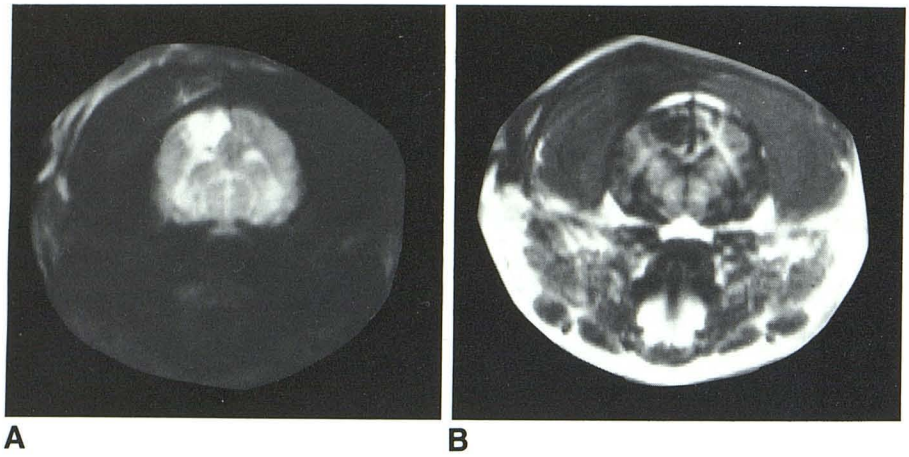

Fig. 1.—Alpha-streptococcus canine brain abscess on day 1 during early cerebritis stage. Unenhanced images at 0.5 T. **A**, SE 2000/120 technique. **B**, IR 1500/450/30 technique.

an 18-gauge burr hole was placed in the left parietal region about 2 cm from the midline. A 25-gauge needle was used to penetrate the dura. A bacteria-agarose mixture (see below) was then injected from a tuberculin syringe at a depth of about 4 mm into the left hemisphere. The inoculum consisted of warm, sterile 1% agarose (0.1 ml) mixed with an equal volume of nutrient broth containing 10^8 colony-forming units. The burr hole was then sealed with bone wax and the incision closed. Each animal was examined at day 1 (24 hr) after surgery (early cerebritis stage) and days 6–8 (late cerebritis stage) by both MR and CT. Due to technical difficulties, one animal was imaged at day 13 (early capsule stage) instead of days 6–8. The animals were secured supine in a specially designed Lucite holder, with the head positioned for coronal scans.

MR Imaging

A Technicare 0.5 T superconducting MR imager was used with a 28 cm internal diameter radiofrequency (RF) coil. The slice thickness was 1.0 cm with a 256 × 256 data matrix and pixel size of 2.2 × 2.2 mm. Before contrast administration, sections were obtained through the area of interest with five different pulse techniques: spin-echo (SE) images using a 500 msec repetition time (TR)/30 msec echo time (TE), 1000 msec TR/120 msec TE, and 2000 msec TR/120 msec TE; inversion-recovery (IR) images using 1500 msec TR/450 msec inversion time (TI)/30 msec TE; and observed T1. The dimethylglucamine salt of Gd DTPA (Schering, West Berlin) was administered as an intravenous bolus at a dose of 0.25 mmol/kg.

SE 500/30 images were then acquired at 2, 10, 30, and 60 min after injection of contrast material, accompanied by observed T1 acquisitions at 25 and 45 min. The signal intensities of normal brain and the area of contrast enhancement were obtained from the SE 500/30 images, using appropriate regions of interest (ROIs). The changes in these parameters after contrast administration, corrected for instrument variation, were computed for each of the five animal groups in both the early and late cerebritis stages. Standard concentrations of Gd DTPA (0.1 and 0.5 mmol), H_2O, and H_2O with 25% D_2O were placed in the field-of-view for each experiment. The signal intensities of these standards were used to follow and correct for scan-to-scan variations.

Calculated T1 and spin-density images were obtained using a two point acquisition method. Two images, an SE 1250/30 sequence and an IR 1250/400/30 technique, were acquired simultaneously. The T1 value was found by fitting the two observed points to a single exponential curve and calculating the time constant for this curve. Mobile proton density, or more simply spin density, was estimated from the upper limit of the exponential curve defined by the OT1 (observed T1) calculation. This computation produces a number that is proportional to proton density, although a slight T2 dependence is induced by T2 dephasing (which occurs during the 30 msec spent generating the SE). Observed T1 values were obtained from normal gray matter, white matter, and brainstem, as well as from the central necrotic abscess and the area of contrast enhancement, using appropriate computer-drawn ROIs.

CT Scanning

Immediately after the MR examination, high-resolution GE 8800 CT/T scans were obtained with and without contrast enhancement (2.2 ml/kg of a 60% meglumine iothalamate solution administered as an intravenous bolus). The CT scanner was operated in the high-resolution infant mode at 120 kVp with sequential 5 mm sections obtained. The repeat scan with enhancement was delayed until 10 min after administration of contrast material. The CT images were then examined for focal areas of low attenuation and abnormal contrast enhancement.

Results

The CT appearance of the brain abscesses correlated well with those described by Enzmann et al. [15]. On postsurgical day 1, a subtle area of low attenuation was noted in three of five cases. Minimal, poorly defined enhancement occurred in four of five cases. By the late cerebritis stage, postsurgical days 6–8, a marked mass effect and ring enhancement were present.

On unenhanced MR examination, the lesions manifested a high signal intensity (long T2) with T2-weighted SE sequences and a low signal intensity (long T1) with T1-weighted IR technique (fig. 1). Lengthening the TR in the SE sequence from 1000 to 2000 msec with TE = 120 msec improved the signal-to-noise (S/N) ratio, as well as contrast between normal and abnormal regions, a result anticipated from previous investigations [18, 19]. However, with such a sequence, cerebrospinal fluid and edema became isointense.

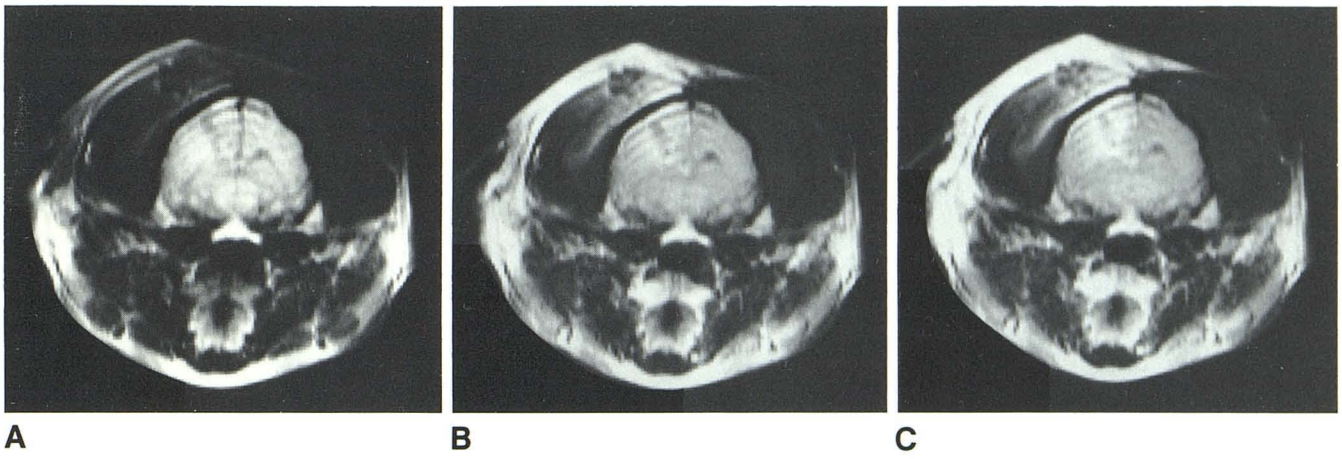

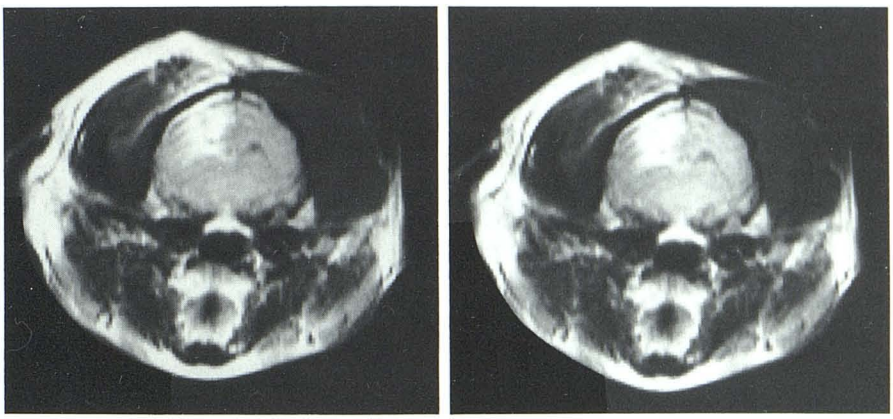

Fig. 2.—SE 500/30 images of brain abscess in fig. before (**A**) and 2 (**B**), 11 (**C**), 35 (**D**), and 62 (**E**) min after bolus intravenous administration of 0.25 mmol/kg Gd DTPA. Contrast enhancement in presumed area of cerebritis, with progressive increase in signal intensity demonstrated up to 1 hr.

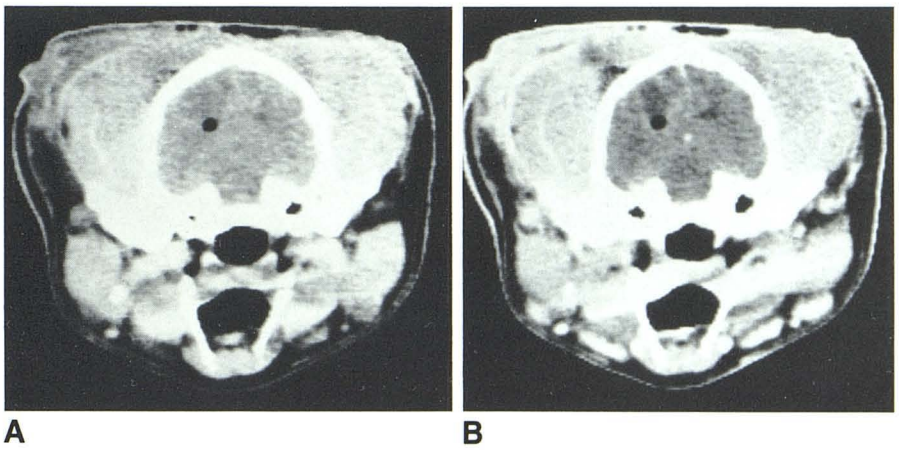

Fig. 3.—High-resolution GE 8800 CT scans of brain abscess in fig. 1 before (**A**) and 10 min after (**B**) bolus intravenous injection of meglumine iothalamate. Minimal, poorly defined enhancement. Intracerebral air, introduced at surgery, is seen on CT and MR (fig. 2).

Enhancement was noted by 2 min postinjection of Gd DTPA and increased in intensity with time, appearing to plateau by 1 hr—the last time point sampled in the current experimentation (fig. 2). Contrast enhancement was consistently greater on the MR examination (at 10 min postadministration) than on the CT scan (fig. 3). The surgical site and mucosa of the nasal sinuses were also consistently noted to increase in signal intensity after administration of contrast material. Examination of the brain abscess with a heavily T1-weighted technique (fig. 4) permitted excellent gray/white-matter discrimination in addition to identification of contrast enhancement. Calculated spin density images changed very little after

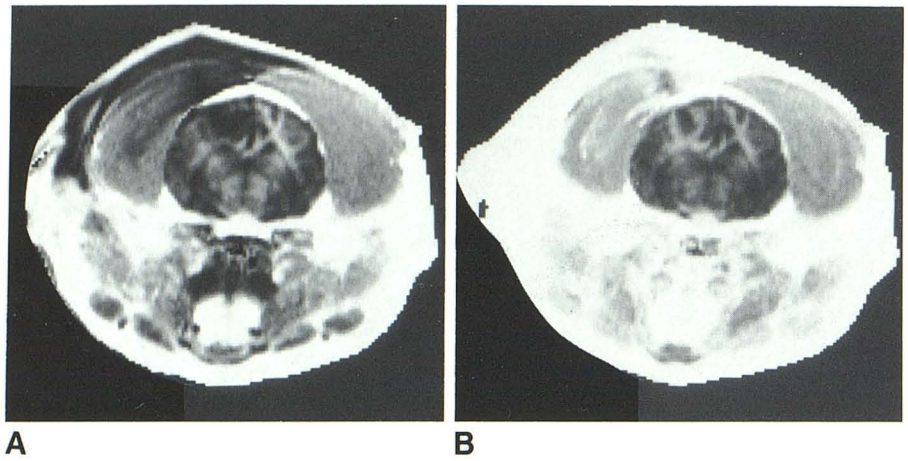

Fig. 4.—Calculated "ratio" images from T1 acquisition sequence before (**A**) and 46 min after (**B**) administration of Gd DTPA in canine brain-abscess model on day 1. Value of each pixel equals value of corresponding pixel on IR 1250/400/30 image divided by that in SE 1250/30 image. These images provide visual representation of T1 information, enabling discrimination of gray matter from white matter and identification of contrast enhancement.

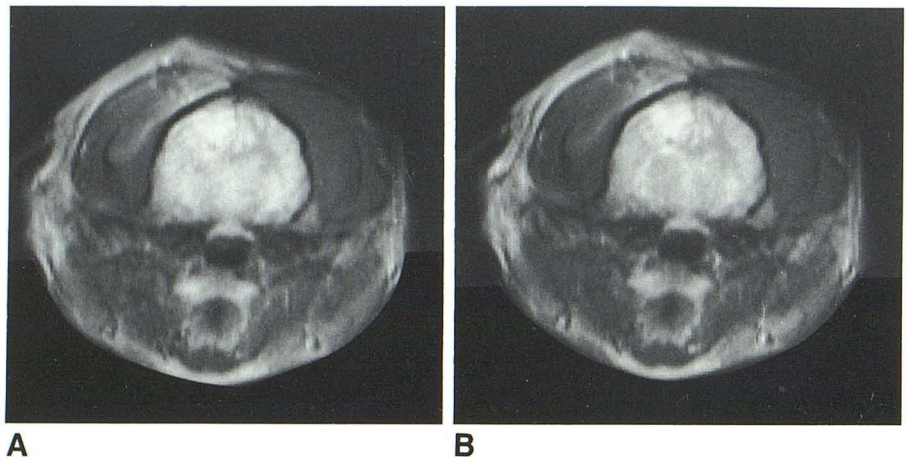

Fig. 5.—Calculated spin density images before (**A**) and 46 min after (**B**) administration of contrast material. Little change in appearance of abscess (early cerebritis stage).

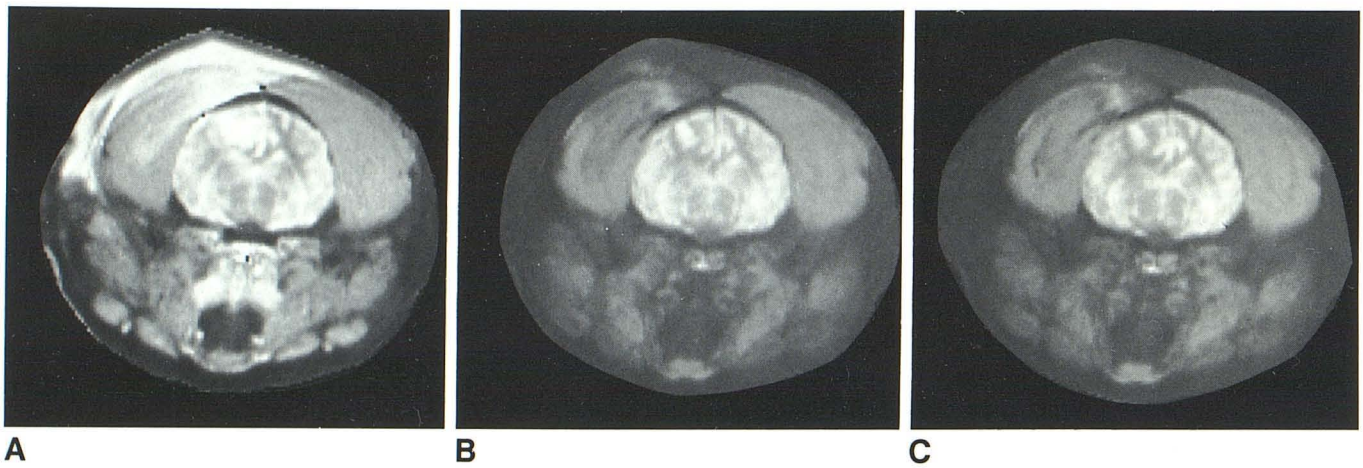

Fig. 6.—Observed T1 images before (**A**) and 25 (**B**) and 46 (**C**) min after intravenous injection of Gd DTPA. Calculated value of T1 decreases in area of contrast enhancement, demonstrated by decrease in brightness on this gray scale (same animal and stage as fig. 1).

administration of contrast material (fig. 5), in sharp distinction to calculated T1 images (fig. 6).

By days 6–8, the lesion had enlarged substantially, and ring enhancement was consistently noted on MR examination (figs. 7–9). With time, the Gd DTPA enhancing ring thickened, eventually filling the lucent center. These changes corresponded well with temporal changes previously described on CT [15].

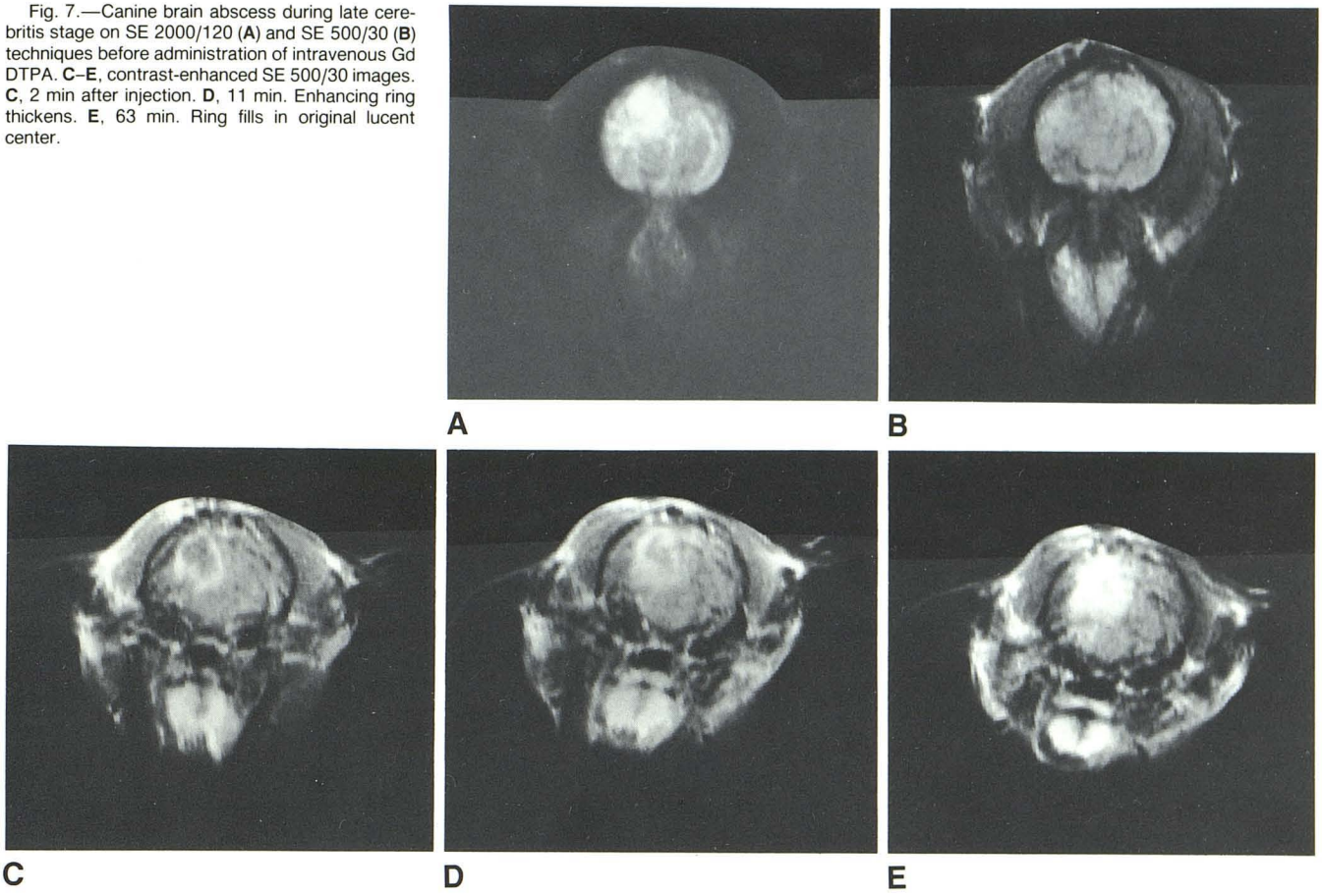

Fig. 7.—Canine brain abscess during late cerebritis stage on SE 2000/120 (**A**) and SE 500/30 (**B**) techniques before administration of intravenous Gd DTPA. **C–E**, contrast-enhanced SE 500/30 images. **C**, 2 min after injection. **D**, 11 min. Enhancing ring thickens. **E**, 63 min. Ring fills in original lucent center.

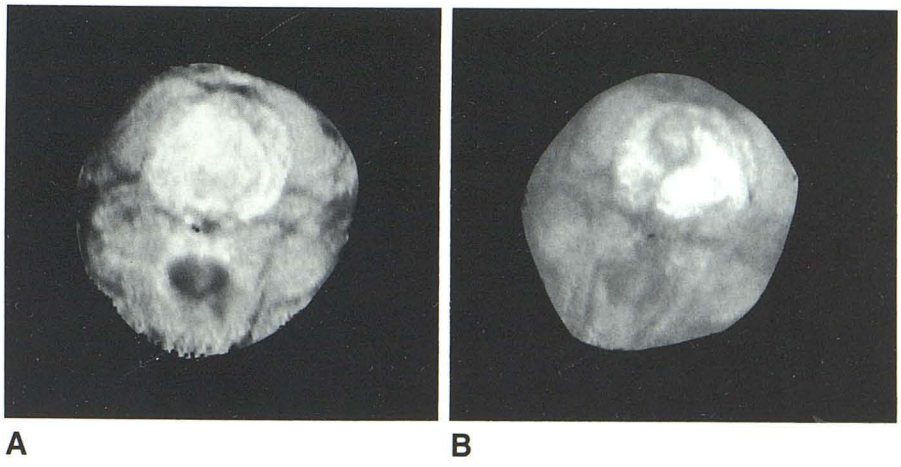

Fig. 8.—Calculated T1 images of late cerebritis abscess (same animal as in fig. 7) before (**A**) and 25 min after (**B**) intravenous administration of Gd DTPA.

The variation in observed T1 of the standards was less than 3% within any experiment. However, a variation of 20% was noted between experiments performed over a 3 month interval. Different coil loading factors and the resultant lack of precise 90° and 180° RF pulses were primarily responsible for this fluctuation. A linear correction was applied to adjust for this variation.

The T1 of normal white matter, gray matter, and brainstem decreased significantly after administration of contrast material (table 1). Although the T1 values of normal brain were consistently lower at 23 min after administration of contrast material when compared with those at 49 min, this difference was only significant ($p < 0.10$) for gray matter.

T1 images demonstrated that the central abscess region

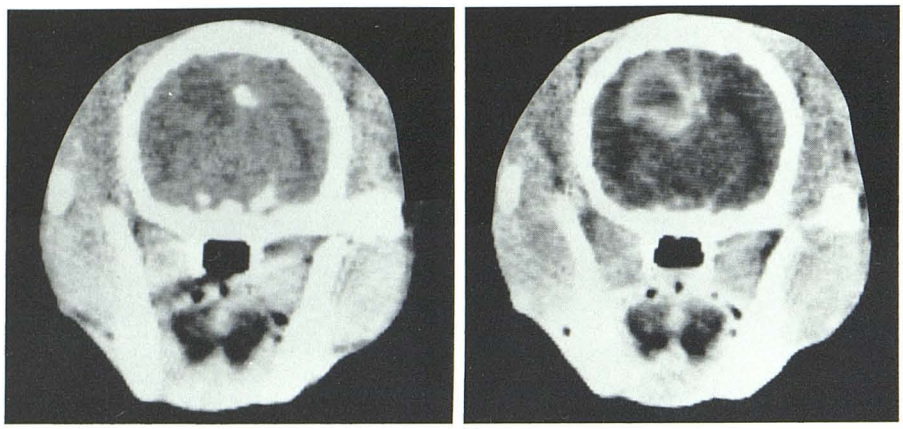

Fig. 9.—GE 8800 CT scans before (**A**) and after (**B**) contrast enhancement with meglumine iothalamate. These images were obtained immediately after MR study fig. 7.

TABLE 1: **Changes Produced in Observed T1 of Normal Brain Components in Dogs by Intravenous Administration of Gd DTPA**

Contrast Parameter	T1 (No. of Dogs)		
	White matter	Gray Matter	Brainstem
Before administration (msec) . .	435.0 ± 48 (12)	546.0 ± 65 (12)	494.0 ± 41 (8)
Decrease after intravenous bolus (%):			
23 min after	4.6 ± 4.1 (7) ($p < 0.025$)	7.4 ± 3.3 (7) ($p < 0.005$)	3.3 ± 1.9 (4) ($p < 0.025$)
49 min after	3.5 ± 2.7 (12) ($p < 0.0005$)	5.3 ± 2.9 (12) ($p < 0.0005$)	2.9 ± 2.6 (8) ($p < 0.01$)

Note.—0.25 mmol/kg of Gd DTPA was injected as an intravenous bolus. Observed T1 values were calculated from MR images obtained at 0.5 T, mean ± SD. Probability (p) values reflect the significance of the change in T1s from their precontrast values.

TABLE 2: **Changes Produced in Observed T1 of the Abscess and "Enhancing Region" in Dogs by Intravenous Administration of Contrast Material**

Contrast Parameter	T1 (No. of Dogs)	
	Area of Enhancement	Central Abscess
Before administration (late cerebritis stage) (msec)	511 ± 63 (4)	601 ± 69 (3)
Decrease after intravenous bolus (%):		
23 min after	29 ± 13 (4) ($p < 0.01$)	28 ± 14 (3) ($p < 0.05$)
50 min after	26 ± 10 (4) ($p < 0.005$)	31 ± 12 (3) ($p < 0.025$)

Note.—p values reflect the significance of the change in T1s from their precontrast values.

TABLE 3: **Comparison of CT and MR Imaging in the Detection of Neurologic Changes in Dogs**

Study	No. of Positive Examinations/Total by Postsurgical Day	
	Day 1	Days 6–13
MR:		
IR 1500/450/30	3/5	3/5
SE 1000/120	3/5	5/5
Contrast enhancement	5/5	5/5
CT:		
Low attenuation	3/5	5/5
Contrast enhancement	4/5	5/5

consistently had a longer T1 value (601 ± 69 msec) than normal gray matter (546 ± 65 msec). Administration of contrast material produced a 28% reduction in T1 in the area of presumed breakdown of the BBB, corresponding to the ring enhancement seen on SE images (table 2). A significant decrease in T1 of the central necrotic region was also observed. This correlated with the time-delayed enhancement of the lucent center on SE images. Two lesions on day 1 (both of which evolved to ring-enhancing lesions by day 8) were detected only by contrast-enhanced MR imaging (table 3).

CT low-attenuation abnormalities on day 1 were subtle. These abnormalities were well defined and clearly separated by their high signal intensity on unenhanced SE 1000/120 examination. Abnormal contrast enhancement occurred on CT in four of the five cases on day 1. However, in only one of these cases was the enhancement more than marginal.

The contrast enhancement demonstrated on MR proved far superior to that on CT, given the doses of contrast material used. No experimental trials were performed in which the administered dose of contrast material was varied. Abnormal

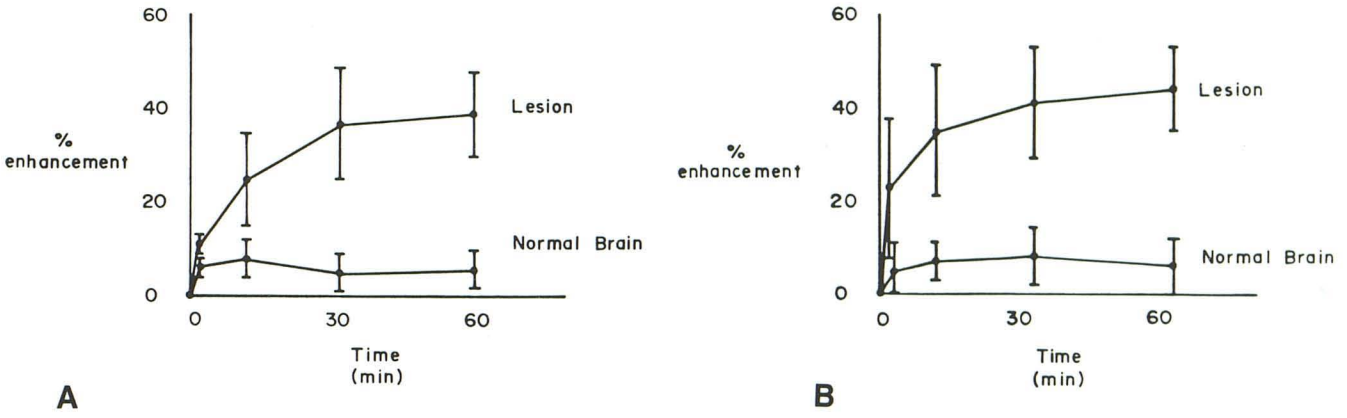

Fig. 10.—Analysis of contrast enhancement on SE 500/30 images produced by intravenous Gd DTPA administration. Each graph summarizes data from five animals. Mean and standard deviations are plotted in early (**A**) and late (**B**) cerebritis stages.

discrete foci of enhancement were identified in all five cases after administration of Gd DTPA. Indeed, in two of the animals, only the contrast-enhanced MR examination demonstrated any abnormality, the unenhanced examination being within normal limits.

Discussion

Proton density, T1, T2, and flow are the four primary variables that determine signal intensity in MR imaging. Using a selected imaging technique, one may manipulate the relative contribution from each factor in an attempt to maximize the diagnostic information obtained. However, until the advent of paramagnetic agents, contrast could not be influenced by the administration of either oral or intravenous materials, as in CT. The iodinated contrast agents of conventional radiology, designed to produce changes in x-ray attenuation, could not be applied to a technique that is primarily dependent on proton resonance.

Two classes of paramagnetic agents have been considered for use in MR imaging: the paramagnetic metal ion chelates [20] and the nitroxide-stable free radicals [21]. Either type of agent can, in addition, be potentially linked to proteins or monoclonal antibodies, creating a more site-specific contrast agent. Through further investigations, Gd DTPA, a member of the first class, was selected as a potential agent for human use. The strong proton relaxation, rapid renal excretion, high in vivo stability, and low toxicity of this agent favor its application to clinical diagnosis.

Paramagnetic agents enhance proton relaxation, shortening both T1 and T2. On SE imaging, this enhancement of T1 relaxation produces an increase in signal intensity and, thus, the desired contrast effect, while the same influence upon T2 is competitive, causing a reduction in signal intensity. With paramagnetic metal ion chelates, the effect on T1 predominates at low concentrations, enabling their use as contrast materials.

The appearance of a brain abscess on MR imaging has been described in three prior publications [12–14], one without contrast enhancement and one, a preliminary report, using a nitroxide-stable free radical. These investigations were limited both by the number of experimental animals and the range of MR pulse techniques used. Our current research used a state-of-the-art, high-field, 0.5 T MR imager and evaluated a compound, Gd DTPA, which is entering phase II clinical studies in Germany.

The CT appearance of the brain abscesses was similar to that previously described [15]. A poorly defined region of low attenuation and minimal irregular enhancement in the early cerebritis stage (postsurgical day 1) consistently evolved to a ring-enhancing lesion with significant mass effect during the late cerebritis stage (days 6–8). Uncontrasted MR imaging was superior to uncontrasted CT scans in the detection and definition of these lesions, which were depicted as areas of high signal intensity on the T2-weighted SE 1000/120 and SE 2000/120 scans. Contrast enhancement with Gd DTPA allowed differentiation of three regions within the lesion: that of the central abscess, the surrounding enhancing rim (presumably corresponding to the area of breakdown of the BBB), and cerebral edema around the abscess. These areas were similarly differentiated on contrast-enhanced CT scans. However, the contrast enhancement noted on MR was consistently greater in degree than that on CT. Furthermore, two early cerebritis lesions were detected only by contrast-enhanced MR imaging. The improved sensitivity of MR to contrast enhancement (with Gd DTPA), when compared with CT, suggests a significant role for contrast-enhanced MR imaging in the detection of neoplastic disease. Small neoplastic foci, primary and metastatic, not detected by CT due to their lack of enhancement, may potentially be identified on contrast-enhanced MR imaging [22].

Use of an IR technique (fig. 4) permitted the visualization of contrast enhancement in addition to the differentiation of gray and white matter. This produced an examination with superior anatomic detail and improved identification of tissue pathology, due to the strong T1-weighting of the image. Comparison of enhanced and unenhanced calculated images demonstrates little change in spin density compared with a dramatic

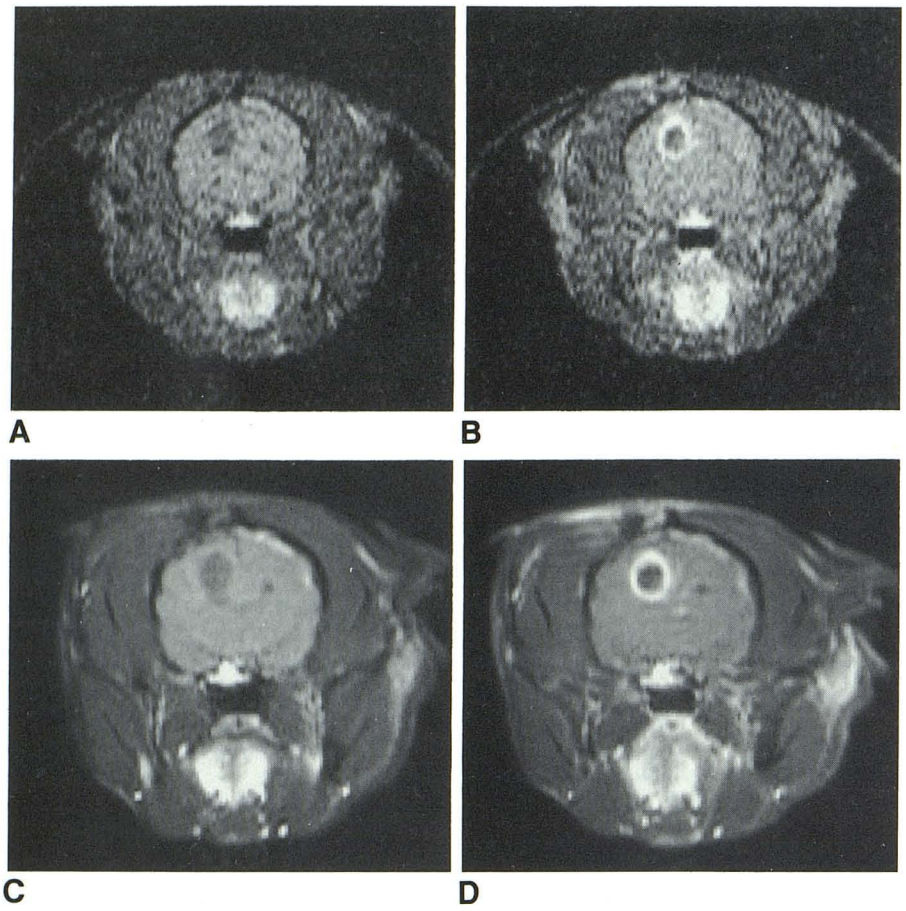

Fig. 11.—Pre- and postcontrast (0.25 mmol/kg Gd DTPA) intravenous MR images of canine brain abscess with SE 250/30 technique. Enhanced scans were obtained 10 min after administration of contrast material. **A** and **B,** 0.15 T (four averages). **C** and **D,** 1.5 T (two averages). Ring enhancement in region of breakdown of BBB.

change in T1. This confirms the primary mechanism of action by which paramagnetic agents alter contrast in MR imaging. These substances act to enhance proton relaxation, the effect upon T1 being particularly important, a conclusion reached from theoretic considerations as well.

The T1 of normal brain tissue decreased by 20–40 msec after intravenous administration of contrast material, although the T1 values at 49 min were slightly greater than those observed at 23 min. These changes presumably reflect a return toward normal T1 values as the agent is cleared by renal excretion. The course of enhancement on SE 500/30 images (fig. 10) was quantitated, with an apparent plateau reached by about 30 min postinjection. The observed time course of enhancement was more rapid for the late, as compared with the early, cerebritis stage. Extrapolation of these data to human studies suggests the utility of delayed scans to maximize contrast enhancement. The mean T1 value of the necrotic center of the abscess decreased by 168 msec 23 min postinjection, presumably reflecting diffusion of contrast material into the interstitial compartment. Ringlike enhancement, theoretically corresponding to an area of altered BBB, occurred in tissue with a lower mean T1 (504 versus 601 msec, corresponding to the necrotic abscess center) before administration of contrast material.

In progress is experimentation designed to evaluate the efficacy of Gd DTPA as a contrast agent in MR imaging over a wide range of magnetic field strengths. Dogs with a late-cerebritis-stage alpha-streptococcus brain abscess were imaged before and after administration of contrast material (0.25 mmol/kg Gd DTPA as an intravenous bolus) at 0.15, 0.5, and 1.5 T. Preliminary findings (fig. 11) reveal the utility of Gd DTPA across the range of field strengths currently available commercially for imaging purposes. The dependence of T1 on magnetic field strengths appears to have little practical importance for the application of Gd DTPA as a contrast agent in MR imaging with the current available range of magnetic fields.

Results from our current investigation indicate that MR imaging may be superior to CT for the detection and characterization of cerebral abscesses, particularly in the early stages of evolution. The greater tissue characterization and the lack of ionizing radiation advocate implementation in neurologic diagnosis. Contrast enhancement with Gd DTPA, a stable, paramagnetic metal ion chelate, permits differentiation of central necrosis in an abscess from surrounding edema. Extrapolation of these results to clinical studies indicates the utility of this agent in the differentiation of neoplastic tissue from cerebral edema and in the identification of other lesions, such as small parasagittal meningiomas, which have been difficult to detect by unenhanced MR.

ACKNOWLEDGMENTS

We thank B. J. Zirger, the CT staff, Bonnie Norman, and John Bobbitt for their help; Mary Henry for editorial assistance; and Technicare Corp. for cooperation.

REFERENCES

1. Bydder GM, Steiner RE, Young IR, et al. Clinical NMR imaging of the brain: 140 cases. *AJNR* **1982**;3:459–480, *AJR* **1982**; 139:215–236
2. Moore WS, Holland GN, Kreel L. The NMR CAT scanner—a new look at the brain. *CT* **1980**;4:1–7
3. Edelstein WA, Hutchison JMS, Smith FW, Mallard J, Johnson G, Redpath TW. Human whole body NMR tomographic imaging: normal sections. *Br J Radiol* **1981**;54:149–151
4. Brant-Zawadzki M, Davis PL, Crooks LE, et al. NMR demonstration of cerebral abnormalities: comparison with CT. *AJNR* **1983**;4:117–124, *AJR* **1983**;140:847–854
5. McGinnis BD, Brady TJ, New PFJ, et al. Nuclear magnetic resonance (NMR) imaging of tumors in the posterior fossa. *J Comput Assist Tomogr* **1983**;7:575–584
6. Kramer DM, Schneider JS, Rudin AM, Lauterbur PC. True three-dimensional nuclear magnetic resonance zeugmatographic images of a human brain. *Neuroradiology* **1981**;21:239–244
7. Modic MT, Weinstein MA, Pavlicek W, et al. Nuclear magnetic resonance imaging of the spine. *Radiology* **1983**;148:757–762
8. Buonanno FS, Pykett IL, Kistler JP, et al. Cranial anatomy and detection of ischemic stroke in the cat by nuclear magnetic resonance imaging. *Radiology* **1982**;143:187–193
9. Alfidi RJ, Haaga JR, El Yousef SJ, et al. Preliminary experimental results in humans and animals with superconducting whole-body NMR scanner. *Radiology* **1982**;143:175–181
10. Brant-Zawadzki M, Badami JP, Mills CM, Normal D, Newton TH. Primary intracranial tumor imaging: a comparison of magnetic resonance and CT. *Radiology* **1984**;150:435–440
11. Runge VM, Clanton JA, Herzer WA, et al. The application of paramagnetic contrast agents to magnetic resonance imaging. *Noninvasive Med Imaging* **1984**;1:137–147
12. Brant-Zawadzki M, Enzmann DR, Placone RC Jr, et al. NMR imaging of experiental brain abscess: comparison with CT. *AJNR* **1983**;4:250–253
13. Brasch RC, Nitecki DE, Brant-Zawadzki M, et al. Brain nuclear magnetic resonance imaging enhanced by a paramagnetic nitroxide contrast agent: preliminary report. *AJNR* **1983**;4:1035–1039, *AJR* **1983**;141:1019–1023
14. Grossman RI, Wolf G, Biery D, et al. Gadolinium enhanced nuclear magnetic resonance images of experimental brain abscess. *J Comput Assist Tomogr* **1984**;8:204–207
15. Enzmann DR, Britt RH, Yeager AS. Experimental brain abscess evolution: computed tomography and neuropathologic correlation. *Radiology* **1979**;133:113–122
16. Weinmann HF, Brasch RC, Press WR, Wesbey GE. Characteristics of gadolinium-DTPA complex: a potential NMR contrast agent. *AJR* **1984**;142:619–624
17. Runge VM, Clanton JA, Lukehart CM, Partain CL, James AE Jr. Paramagnetic agents for contrast-enhanced NMR imaging: a review. *AJR* **1983**;141:1209–1215
18. Crooks LE, Hoenninger J, Arakawa M, et al. High-resolution magnetic resonance imaging: technical concepts and their implementation. *Radiology* **1984**;150:163–171
19. Runge VM, Price AC, Kirshner HS, Allen JH, Partain CL, James AE Jr. Magnetic resonance imaging of multiple sclerosis: a study of pulse-technique efficacy. *AJNR* **1984**;5:691–702, *AJR* **1984**;143:1015–1026
20. Runge VM, Stewart RG, Clanton JA, et al. Work in progress: potential oral and intravenous paramagnetic NMR contrast agents. *Radiology* **1983**;147:789–791
21. Brasch RC, London DA, Wesbey GE, et al. Work in progress: nuclear magnetic resonance study of a paramagnetic nitroxide contrast agent for enhancement of renal structures in experimental animals. *Radiology* **1983**;147:773–779
22. Runge VM, Schorner W, Niendorf HP, et al. Initial clinical evaluation of gadolinium DTPA for contrast-enhanced magnetic resonance imaging. *Magnetic Resonance Imaging* (in press)